Articles

Rotational Dynamics of Actin-Bound Intermediates in the Myosin ATPase Cycle†

Christopher L. Berger‡ and David D. Thomas*
Department of Biochemistry, University of Minnesota Medical School, Minneapolis, Minnesota 55455
Received April 12, 1991; Revised Manuscript Received August 27, 1991

ABSTRACT: We have used saturation-transfer electron paramagnetic resonance (ST-EPR) to detect the microsecond rotational motions of spin-labeled myosin subfragment one (MSL-S1) bound to actin in the presence of the ATP analogues AMPPNP (5′-adenylylimido diphosphate) and ATPγS [adenosine 5′-*O*-(3-thiotriphosphate)], which are believed to trap myosin in strongly and weakly bound intermediate states of the actomyosin ATPase cycle, respectively. Sedimentation binding measurements were used to determine the fraction of myosin heads bound to actin under ST-EPR conditions and the fraction of heads containing bound nucleotide. ST-EPR spectra were then corrected to obtain the spectrum corresponding to the ternary complex (actin·MSL-S1·nucleotide). The ST-EPR spectrum of MSL-S1·AMPPNP bound to actin is identical to that obtained in the absence of nucleotide (rigor complex), indicating no rotational motion of MSL-S1 relative to actin on the microsecond time scale. However, MSL-S1·ATPγS bound to actin is rotationally mobile, with an effective rotational correlation time (τ_r) of 17 ± 2 μs. This motion is similar to that observed previously for actin-bound MSL-S1 during the steady-state hydrolysis of ATP [Berger et al. (1989) *Proc. Natl. Acad. Sci. U.S.A. 86*, 8753–8757]. We conclude that, in solution, the weakly bound actin-attached states of the myosin ATPase cycle undergo microsecond rotational motions, while the strongly bound intermediates do not, and that these motions are likely to be involved in the molecular mechanism of muscle contraction.

The molecular mechanism of muscle contraction is postulated to involve the repeating cyclic interaction of actin and myosin (the two major protein components of muscle), whereby force is generated when the head of the myosin molecule (subfragment one, S1)[1] rotates while bound to actin (Huxley, 1969; Huxley & Simmons, 1971; Huxley, 1974; Huxley & Kress, 1985). This proposed process is tightly coupled to the hydrolysis of ATP (the major source of chemical energy in muscle) by S1, and specific states of the actomyosin ATPase cycle are thought to mediate the interaction between actin and myosin (Lymn & Taylor, 1971; Eisenberg & Hill, 1985). While this model has been supported by structural, mechanical, and biochemical studies over the past 30 years, direct evidence for the rotation of S1 relative to actin during the contractile cycle has remained elusive.

Spectroscopic molecular probes provide a means by which the orientation and rotational motions of specifically labeled muscle proteins can be directly monitored [reviewed by Thomas (1987)]. Previous work using electron paramagnetic resonance (EPR) to measure orientation, and saturation-transfer EPR (ST-EPR) to measure microsecond rotational motions, has demonstrated that most of the myosin heads (>80%) in an isometrically contracting muscle fiber are highly disordered (Cooke et al., 1982; Fajer et al., 1990b) and mobile on the microsecond time scale (Barnett & Thomas, 1989). Additionally, time-resolved phosphorescence has shown that isometrically contracting muscle fibers undergo rotational motions that are distinct from those in rigor (no nucleotide) or relaxation (Stein et al., 1990). Stiffness is not necessarily a linear function of actin-attached myosin heads (cross-bridges), and it is difficult to determine unambiguously the fraction of attached cross-bridges in complex contractile systems such as myofibrils and muscle fibers (Pate & Cooke, 1988; Fajer et al., 1988). Thus, even though the stiffness in an isometrically contracting muscle fiber is high (70–80% of the rigor value), the contribution of the attached cross-bridges to the observed spectroscopic signals is unclear.

The ambiguity of cross-bridge attachment can be avoided by using solutions of S1 covalently cross-linked to actin (XLAS1). ST-EPR experiments on spin-labeled XLAS1 have shown that the myosin heads undergo microsecond rotational motions during steady-state ATP hydrolysis (Svensson & Thomas, 1986), but it is not clear that myosin heads covalently cross-linked to actin are a true analogue of physiologically attached cross-bridges. However, the fraction of uncross-linked S1 bound to actin in solution (acto-S1) can be determined directly from sedimentation experiments (Chalovich & Eisenberg, 1982), making it possible to analyze the rotational motion of the actin-attached myosin heads explicitly in the case of acto-S1. We have previously established, using ST-EPR and sedimentation experiments, that spin-labeled S1 (MSL-S1) undergoes microsecond rotational motions while

† This work was supported by grants from the National Institutes of Health (AR32961 and RR03826) and the Minnesota Supercomputer Institute. C.L.B. was supported by a Training Grant from the National Institutes of Health and a Doctoral Dissertation Fellowship from the University of Minnesota.
* To whom correspondence should be addressed.
‡ Present address: Pennsylvania Muscle Institute, University of Pennsylvania School of Medicine, Philadelphia, PA 19104.

[1] Abbreviations: ADP, adenosine 5′-diphosphate; ATP, adenosine 5′-triphosphate; caged ATP, the P^3-1-(2-nitrophenyl)ethyl ester of ATP; AMPPNP, 5′-adenylylimido diphosphate; ATPγS, adenosine 5′-*O*-(3-thiotriphosphate); S1, myosin subfragment one; HMM, heavy meromyosin; MSL, 4-maleimido-2,2,6,6-tetramethyl-1-piperinyloxy; EPR, electron paramagnetic resonance; ST-EPR, saturation-transfer electron paramagnetic resonance; SEM, standard error of the mean; EGTA, ethylene glycol bis(β-aminoethyl ether)-*N*,*N*,*N*′,*N*′-tetraacetic acid; $MgCl_2$, magnesium chloride; KPr, potassium propionate; TEAB, triethylamine bicarbonate.

0006-2960/91/0430-11036$02.50/0

bound to actin during steady-state ATP hydrolysis (Berger et al., 1989). Conditions of low ionic strength and high actin concentration were used to ensure that a significant fraction of the MSL-S1 was bound to actin. Complementary experiments with the spin label attached to actin instead of S1 indicate that the myosin heads rotate relative to actin under these conditions (Ostap & Thomas, 1991).

In the present study, in order to determine which attached states of the actomyosin ATPase cycle correspond to the mobile actin-attached population of myosin heads observed during the steady-state hydrolysis of ATP, we have used the ATP analogues AMPPNP (5′-adenylylimido diphosphate) and ATPγS [adenosine-5′-*O*-(3-thiotriphosphate)] to trap MSL-S1 in states that are thought to correspond to the two major conformational intermediates of the actomyosin ATPase cycle. These two major conformational states of myosin, which have been identified both through structural (Shriver & Sykes, 1981, 1982; Barnett & Thomas, 1987) and kinetic (Geeves et al., 1984; Eisenberg & Hill, 1985) means, are often referred to as the weakly bound and strongly bound intermediates of the actomyosin ATPase cycle. In the presence of AMPPNP, a nonhydrolyzable analogue of ATP (Yount et al., 1971a,b), muscle fibers exhibit structural (Barrington-Leigh et al., 1972; Goody et al., 1975; Lymn, 1975; Marston et al., 1976; Padron & Huxley, 1984; Fajer et al., 1988) and mechanical [Marston et al. (1976), reviewed by Kuhn (1981)] properties intermediate between those of rigor and relaxation, and myosin is believed to be trapped in a strongly bound intermediate state of the ATPase cycle (Greene & Eisenberg, 1978). ATPγS, an analogue of ATP that is hydrolyzed 500 times more slowly than ATP (Bagshaw et al., 1972; Barrington-Leigh et al., 1972), is thought to accumulate myosin in a weakly bound prehydrolysis intermediate state of the ATPase cycle (Goody & Hofmann, 1980). We have used ST-EPR to measure the microsecond rotational motions of MSL-S1 bound to actin in the presence of AMPPNP or ATPγS, at low and physiological ionic strengths. The fraction of actin-attached myosin heads in the presence of either AMPPNP or ATPγS has been determined from sedimentation experiments and used to determine directly the ST-EPR spectra of the ternary complexes actin·MSL-S1·nucleotide. Thus we were able to measure the microsecond rotational motions of MSL-S1 bound to actin in possible intermediate states of the actomyosin ATPase cycle.

Materials and Methods

Preparations and Solutions. Chymotryptic myosin subfragment one (S1) was prepared as described previously (Eads et al., 1984), except that the chymotryptic digestion time was 10 min. S1 was spin-labeled at SH-1 (Cys-707) with 4-maleimido-2,2,6,6-tetramethyl-1-piperinyloxy (MSL; Aldrich) to the extent of 0.98 ± 0.02 label bound per head, with a specificity of 1.00 ± 0.04, as previously described (Svensson & Thomas, 1986). The concentrations of S1 and MSL-labeled S1 (MSL-S1) were determined spectrophotometrically at 280 nm, using an extinction coefficient of 0.75 $(mg/mL)^{-1}$ cm^{-1}. The spin concentration was determined by double integration of the digitized low-power conventional EPR spectrum (Squier & Thomas, 1986). F-actin was prepared as previously described (Thomas et al., 1979). The concentration of G-actin was determined spectrophotometrically at 290 nm, using an extinction coefficient of 0.63 $(mg/mL)^{-1}$ cm^{-1}. The tetralithium salts of AMPPNP (5′-adenylylimido diphosphate) and ATPγS [adenosine 5′-*O*-(3-thiotriphosphate)] were purchased from Boeringer-Mannheim. The nucleotides were purified by HPLC on a preparative Bio-Rad MA7Q anion exchange column (2 cm × 10 cm) and eluted with a linear gradient of 0–1.0 M triethylamine bicarbonate (TEAB), pH 7.8. The eluted nucleotides were then lyophilized, resuspended in distilled water, lyophilized again, and diluted to a final concentration of 100–150 mM in low ionic strength buffer (10 mM imidazole, 1 mM EGTA, pH 7.0). The purified nucleotide concentration was determined spectrophotometrically at 259 nm, using an extinction coefficient of 15.1 mM^{-1} cm^{-1}. The amount of ATPγS hydrolyzed during the ST-EPR and sedimentation binding experiments was determined by measuring the rate of inorganic phosphate production according to the method of Lanzetta et al. (1979). Experimental conditions are defined as 10 mM imidazole, 2 mM EGTA, and 2 mM $MgCl_2$ (pH 7.0), plus the indicated concentration of magnesium nucleotide (AMPPNP or ATPγS). Potassium propionate (KPr) was added to achieve the desired ionic strength.

Our primary goal in these studies was to obtain EPR spectra of the ternary complexes actin·MSL-S1·nucleotide, so conditions were chosen to maximize the binding of actin and nucleotides to S1, and these conditions were used for both EPR and actin-binding measurements. For ATPγS, we chose the same conditions, 5 mM nucleotide, low ionic strength (36 mM), and high actin concentration (200 μM), that had been used previously to study MSL-S1 bound to actin during steady-state ATP hydrolysis (Berger et al., 1989). We used similar conditions in the presence of AMPPNP, except that the weaker nucleotide affinity required a higher (16 mM) AMPPNP concentration, resulting in a higher minimum ionic strength (100 mM). Experiments were also performed at physiological ionic strength (μ = 186 mM).

Sedimentation Binding Experiments. The apparent association constant (K_{app}) for MSL-S1 binding to actin was measured by sedimenting a 200-μL sample of actin and/or MSL-S1 in a Beckman TL-100 centrifuge for 10 min at 386000*g* at 25 °C in order to pellet the actin and actin-bound MSL-S1. The resulting supernatants (sup) were assayed for protein concentration ([protein]) using the enhanced protocol of the BCA protein assay (Pierce), and these values were compared to controls containing no actin in order to determine the fractions of free (f_F) and actin-bound (f_B) MSL-S1:

$$f_F = (\text{[protein] in acto-S1 sup})/(\text{[protein] in S1 sup}) \quad (1)$$

and

$$f_B = 1 - f_F \quad (2)$$

K_{app} was then determined from f_B, f_F, and the initial MSL-S1 ([S1]) and actin ([A]) concentrations:

$$K_{app} = f_B[S1]/f_F[S1]([A] - f_B[S1]) \quad (3)$$

Sedimentation binding samples contained 10 μM MSL-S1 and 40 μM actin in the presence of 0–16 mM AMPPNP, and 100 μM MSL-S1 and 200 μM actin in the presence of 0–5 mM ATPγS. Binding experiments were also performed with 100 μM MSL-S1 and 200 μM of actin in the presence of 16 mM AMPPNP, in order to ensure that the observed binding constant was not altered by the high concentrations of protein required by the spectroscopy experiments. Lower concentrations of MSL-S1 and actin were also used in the Scatchard analysis of acto-S1 binding in the presence of low AMPPNP concentrations (12 μM actin, 3–24 μM MSL-S1 at 0.5 mM AMPPNP; 16 μM actin, 4–32 μM MSL-S1 at 1.0 mM AMPPNP; 20 μM actin, 5–40 μM MSL-S1 at 2.0 mM AMPPNP). K_{app} was determined in the Scatchard analysis experiments from a linear least-squares best fit of the data using

$$[S1_{bound}]/([S1_{free}][A_{total}]) = -K_{app}([S1_{bound}]/[A_{total}]) + K_{app} \quad (4)$$

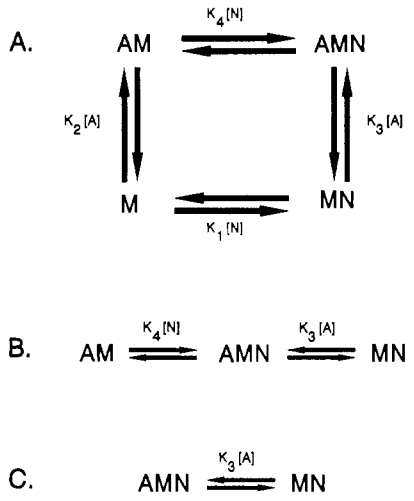

FIGURE 1: Interaction between MSL-S1 (M), actin (A), and nucleotide (N). A. General binding scheme. B. Simplified binding scheme assuming K_1 and K_2 are sufficiently strong that MSL-S1 is always bound to actin, nucleotide, or both. C. Simplified binding scheme assuming K_1 and K_4 are sufficiently strong that MSL-S1 always has nucleotide bound.

Samples containing 200 μM actin in the absence of MSL-S1 were sedimented as a control for unpolymerized actin.

The evaluation of K_{app} depends on the relative interactions between MSL-S1 (M), actin (A), and nucleotide (N), as depicted by the binding scheme in Figure 1A. This binding scheme can be simplified if A and N both bind strongly enough to M, such that all M is bound to A, N, or both. In this case, the binding scheme in Figure 1A simplifies to the one in Figure 1B, and K_{app} can be defined as a function of both the binding constant of A to MN (K_3) and the binding constant of N to AM (K_4) (Biosca et al., 1986):

$$K_{app} = (K_3/K_4)(1/[N]) + K_3 \quad (5)$$

Thus by measuring K_{app} over a range of [N] and plotting K_{app} vs $1/[N]$, K_3 and K_4 can be determined from a linear least-squares fit to the data. The fraction of M with bound N [f_N = ([MN] + [AMN])/[AM]] or bound A [f_A = ([AM] + [AMN])/[MN]], can be determined from K_3 or K_4 and the total concentrations of M, A, and N:

$$f = [b - (b^2 - 4ac)^{1/2}]/2a \quad (6)$$

where $a = K_3[M]_{tot}$ or $K_4[M]_{tot}$, $b = a + c + 1$, and $c = K_3[A]_{tot}$ or $K_4[N]_{tot}$. The binding scheme in Figure 1B can be further simplified to the one in Figure 1C if N binds strongly to AM, such that [AM] = 0. In this case $K_3 = K_{app}$, which is determined directly from the sedimentation experiments, using eq 3.

EPR Experiments and Data Analysis. EPR and ST-EPR spectra were obtained as described previously (Squier & Thomas, 1986) using a Bruker ESP 300 spectrometer equipped with a TE_{102} cavity (Bruker model ER4102ST) and a quartz Dewar insert. Conventional EPR (V_1) spectra were obtained using 100 kHz field modulation (with a peak-to-peak modulation amplitude of 2 G), with a microwave field intensity (H_1) of 0.032 G. ST-EPR (V'_2) spectra were obtained using 50 kHz field modulation (with a peak-to-peak modulation amplitude of 5 G), with a microwave field intensity (H_1) of 0.25 G. The sample was contained in a 25-μL gas-permeable TPX capillary (1.0-mm internal diameter), allowing the removal of dissolved oxygen by purging the samples with nitrogen (Squier & Thomas, 1986). The temperature was maintained at 25 ± 0.5 °C by flowing precooled N_2 over the sample, which was regulated by a variable temperature controller (Bruker model ER4111). All ST-EPR spectra (V'_2) were normalized by dividing by the double integral of the low-power (H_1 = 0.032 G) conventional EPR spectrum (V_1), a parameter that is independent of rotational motion and corrects for any variation in the concentration of spin labels between samples (Squier & Thomas, 1986). All ST-EPR samples contained 100 μM MSL-S1, 200 μM actin (if present), and 16 mM AMPPNP or 5 mM ATPγS (if nucleotide was present). The high concentration (100 μM) of MSL-S1 used was required for adequate signal intensity in the ST-EPR experiments.

Digitized EPR spectra were acquired with the spectrometer's built-in microcomputer using Bruker OS-9-compatible ESP 1620 spectral acquisition software and then were transferred to an IBM-compatible microcomputer and analyzed using a program developed by Robert L. H. Bennett. A total of 9–16 scans were acquired per ST-EPR spectrum and digitally averaged. Effective rotational correlation times (τ_r) were determined from the ST-EPR spectra using calibration curves of the line-height ratio parameter C'/C and the normalized intensity parameter ($\int V'_2/\int\int V_1/H_1$), which were derived from spin-labeled hemoglobin samples with known rotational correlation times (Thomas, et al., 1976; Squire & Thomas, 1986).

S_{AMN}, the ST-EPR spectrum of the ternary complex AMN (i.e., actin·MSL-S1·nucleotide) was derived from S_{total} (the composite spectrum observed in the presence of A, M, and N), and the ST-EPR spectra of the rigor actin·S1 complex (AM) and the free S1·nucleotide complex (MN), from the following relationship:

$$S_{total} = f_M S_M + f_{MN} S_{MN} + f_{AMN} S_{AMN} + f_{AM} S_{AM} \quad (7)$$

where S_i and f_i are the spectrum and mole fraction of species i. Under our experimental conditions, $F_M = 0$, so the spectrum of the ternary complex is

$$S_{AMN} = (S_{total} - f_{MN} S_{MN} - f_{AM} S_{AM})/f_{AMN} \quad (8)$$

The mole fractions f_A and f_N are determined from sedimentation data and eq 6; then $f_{AM} = 1 - f_N$, $f_{AMN} = f_N f_A$, and $f_{MN} = 1 - f_{AM} - f_{AMN}$. If the nucleotide binding to AM is strong enough that $f_{AM} = 0$ (achieved below for ATPγS but not for AMPPNP), eq 8 can be simplified to

$$S_{AMN} = [S_{total} - S_{MN}(f_{MN})]/(f_{AMN}) \quad (9)$$

where f_{MN} and f_{AMN} are now equivalent to the fraction of free (f_F) and bound (f_B) heads determined directly from the sedimentation experiments (eqs 1 and 2).

RESULTS

Sedimentation Experiments. Sedimentation binding experiments were performed in order to determine the fraction of MSL-S1 bound to actin and to nucleotide. These results are summarized in Table I. S1 binds to actin very strongly in the absence of nucleotide (rigor), with an association constant greater than 10^7 M^{-1} even at high ionic strength (Greene & Eisenberg, 1980a). We verified that essentially all of the MSL-S1 is bound to actin (0.98 ± 0.01) in the absence of nucleotide under our experimental conditions (data not shown). It has been demonstrated previously that AMPPNP (Greene & Eisenberg, 1980a) and ATPγS (Bagshaw et al., 1972) bind very strongly to S1, with association constants of 1.5×10^6 M^{-1} and at least 10^7 M^{-1}, respectively. Thus the general binding scheme in Figure 1A can be simplified to the one in Figure 1B, and K_3 and K_4 can be determined from a plot of K_{app} vs $1/[N]$ (eq 5).

The fraction of MSL-S1 bound to actin was measured over a range of AMPPNP concentrations (0.5–16 mM). K_{app} was

Table I: MSL-S1 Binding Parameters Determined from Sedimentation Experiments[a]

nucleotide (mM)	K_3 (M^{-1})	f_A	K_4 (M^{-1})	f_N	f_B
AMPPNP[b]					
μ = 100	(2.23 ± 0.42) × 10^4	0.74 ± 0.03	(3.32 ± 0.16) × 10^2	0.84 ± 0.01	0.76 ± 0.04
μ = 186	(2.51 ± 0.72) × 10^3	0.30 ± 0.05	(3.15 ± 0.18) × 10^2	0.83 ± 0.01	0.42 ± 0.03
ATPγS[c]					
μ = 36	(2.22 ± 0.38) × 10^3	0.27 ± 0.04	>1.0 × 10^4	>0.98	0.27 ± 0.03
μ = 186	<1.0 × 10^2	<0.02	>1.0 × 10^4	>0.98	0.00 ± 0.02

[a] K_3 is the association constant for the binding of MN (MSL-S1·nucleotide) to A (actin), and K_4 is the association constant for the binding of N to AM (see Figure 1). f_A is the fraction of total MN that is bound to A, as determined from K_3 and eq 5, and f_N is the fraction of total M with bound N, as determined from K_4 and eq 5. f_B is the fraction of total M that is bound to A, measured directly from sedimentation experiments under ST-EPR conditions. All errors are given as SEM, n = 4–8. [b] For AMPPNP, K_3 and K_4 were determined using linear regression analysis from plots of K_{app} vs 1/[AMPPNP]. [c] For ATPγS, f_A and F_N were determined directly from sedimentation experiments in the presence of ATPγS and were used to determine the upper and lower limits for K_3 and K_4, respectively.

Table II: ST-EPR Spectral Parameters and Effective Rotational Correlation Times[a]

	composite spectra		bound S1[b]	
	C'/C	τ_r (μs)	C'/C	τ_r (μs)
controls[c]				
MSL-S1	−0.83 ± 0.10	0.35 ± 0.12		
actin + MSL-S1	0.76 ± 0.04	104 ± 14	0.76 ± 0.04	104 ± 14
AMPPNP				
actin + MSL-S1 (μ = 100 mM)	0.35 ± 0.06	24.5 ± 5.5	0.79 ± 0.02	115 ± 7
actin + MSL-S1 (μ = 186 mM)	0.03 ± 0.08	8.0 ± 2.3	0.79 ± 0.01	114 ± 5
ATPγS				
actin + MSL-S1 (μ = 36 mM)	−0.21 ± 0.12	3.7 ± 1.8	0.25 ± 0.02	17.1 ± 1.5
actin + MSL-S1 (μ = 186 mM)	−0.78 ± 0.02	0.42 ± 0.08		

[a] C'/C is the standard line-height ratio parameter from the center of the ST-EPR spectrum (Thomas et al., 1976; Squier & Thomas, 1986). τ_r is the effective rotational correlation time in microseconds calculated from C'/C. All errors are given as SEM, n = 5–9. [b] Bound S1 is the ternary complex (A·M·N) bound to both nucleotide and actin. [c] Results are averaged together for the MSL-S1 spectra, regardless of ionic strength or the nucleotide present, and for the actin + MSL-S1 (rigor) spectra, regardless of ionic strength.

determined at each concentration of AMPPNP in these experiments and plotted versus 1/[AMPPNP] in order to determine K_3 and K_4. Scatchard plots were used to determine K_{app} at low [AMPPNP] (≤2 mM), using lower concentrations of actin. From a linear least-squares fit to eq 5, K_3 was determined to be (2.23 ± 0.42) × 10^4 M^{-1}, and K_4 was determined to be (3.32 ± 0.16) × 10^2 M^{-1} and MSL-S1, actin, and AMPPNP. The fraction of MSL-S1 bound to actin and/or AMPPNP in the presence of 16 mM AMPPNP at the protein concentrations used in the ST-EPR experiments (100 μM MSL-S1, 200 μM actin) was determined from the calculated values of K_3 and K_4 (eq 6). These calculations showed that 78 ± 4% of the MSL-S1 was bound to actin, 62 ± 4% with AMPPNP bound (ternary complex, AMN), and 16 ± 1% without nucleotide bound (rigor, AM). The remaining 22 ± 2% of the MSL-S1 (MN) was not bound to actin. These results agree with sedimentation binding experiments, which directly measured the fraction of bound MSL-S1 to be 0.76 ± 0.04 under the ST-EPR experimental conditions.

At physiological ionic strength (μ = 186 mM) it was possible to determine K_{app} over a higher range of AMPPNP concentrations (4–32 mM) than could be used at the lower ionic strength (μ = 100 mM). Under these conditions, from a plot of K_{app} vs 1/[AMPPNP], K_3 and K_4 were determined to be 2.51 × 10^3 M^{-1} and 3.15 × 10^2 M^{-1}, respectively. Therefore, under the ST-EPR experimental conditions (100 μM MSL-S1, 200 μM actin, 16 mM AMPPNP) at physiological ionic strength, it was calculated that 42 ± 5% of the MSL-S1 was bound to actin, 25 ± 4% with AMPPNP bound (AMN), and 17 ± 1% without nucleotide bound (AM). The remaining 58 ± 2% of the MSL-S1 (MN) was not bound to actin. These results agree closely with sedimentation binding measurements, which directly measured the fraction of MSL-S1 bound to actin to be 0.42 ± 0.03 under the ST-EPR experimental conditions.

Due to the weak binding of MSL-S1 to actin in the presence of ATPγS, even at low ionic strength (μ = 36 mM), K_{app} was determined at the high protein concentrations used in the ST-EPR experiments (100 μM MSL-S1, 200 μM actin), ensuring that a significant fraction of MSL-S1 was bound to actin under these conditions. The value of K_{app} was independent of [ATPγS] over the concentration range used (0.5–5.0 mM), indicating that [ATPγS] was sufficient for saturation. Thus in the presence of ATPγS at low ionic strength, the binding scheme in Figure 1C is valid, and the measured value of K_{app} is equivalent to K_3. The fraction of MSL-S1 bound to actin (as the ternary complex AMN) under these conditions was determined to be 0.27 ± 0.03, corresponding to a value of (2.22 ± 0.38) × 10^3 M^{-1} for K_3. At physiological ionic strength (μ = 186 mM), the binding of MSL-S1 to actin in the presence of ATPγS was too weak to be measured (K_3 < 1.0 × 10^2 M^{-1}) even at the high protein concentrations used in the ST-EPR experiments (100 μM MSL-S1, 200 μM actin), and essentially none (0.00 ± 0.02) of the MSL-S1 was bound to actin. The accumulation of ADP was not a limiting factor in the sedimentation binding or ST-EPR experiments, since the rate of ATPγS hydrolysis by acto-MSL-S1 was determined to be quite slow (0.008 ± 0.006 s^{-1}) under the conditions used.

ST-EPR Experiments. Effective rotational correlation times (τ_r) determined from ST-EPR spectra, using the C'/C line-height ratio parameter, are summarized in Table II. The τ_r values determined from the normalized intensity parameter ($\int V'_2/\int\int V_1/H_1$; Squier & Thomas, 1986) were not significantly different (data not shown). The ST-EPR spectrum of the ternary complex, actin·MSL-S1·nucleotide (AMN), was obtained as indicated in eq 8 in the presence of AMPPNP, or eq 9 in the presence of ATPγS.

The ST-EPR spectrum of MSL-S1 (Figure 2, center column) is independent of the nucleotide present. The effective

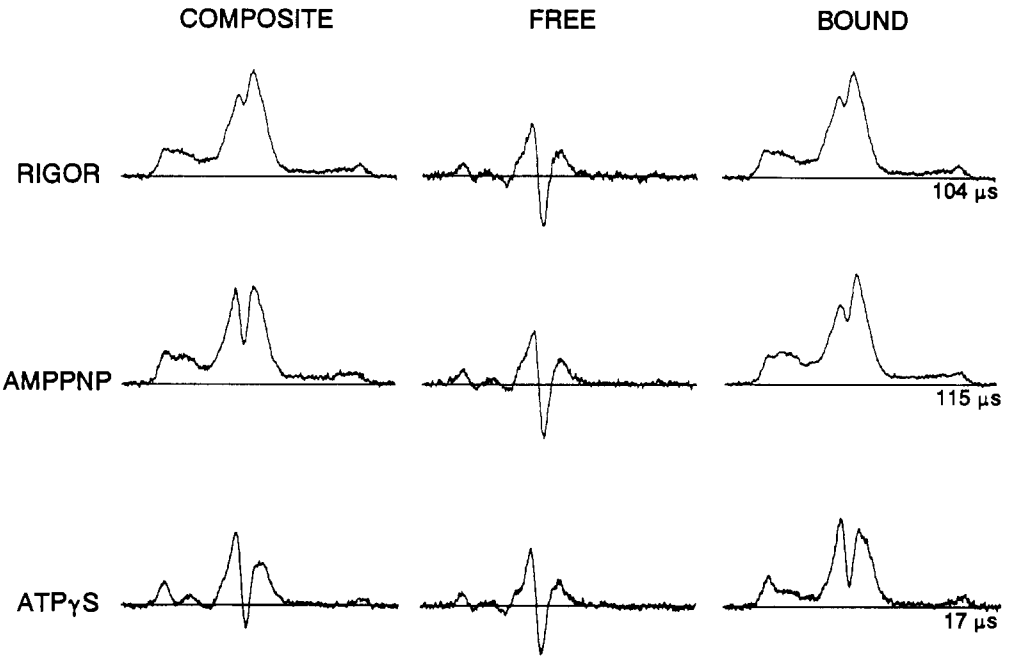

FIGURE 2: ST-EPR spectra of 100 μM MSL-S1 + 200 μM actin (left), 100 μM MSL-S1 (center), and actin-bound MSL-S1 (right) in the absence of nucleotide (first row, μ = 36 mM), and in the presence of 16 mM AMPPNP (second row, μ = 100 mM) or 5 mM ATPγS (third row, μ = 36 mM), at 25 °C. The spectrum of the actin-bound MSL-S1 (right) was obtained by subtracting the appropriate mole fraction of the free MSL-S1 spectrum (center) from the composite spectrum (left). In the presence of AMPPNP, since the MSL-S1 was not completely saturated with AMPPNP, an additional correction was made by subtracting the appropriate mole fraction of the rigor spectrum from the composite spectrum. Thus the spectra of the bound components correspond to the ternary complexes actin·MSL-S1·nucleotide (AMN in Figure 1 and eqs 8 and 9). The numbers below spectra are effective rotational correlation times (τ_r), determined from C'/C. Each spectral baseline is 100 G wide.

rotational correlation time (τ_r = 0.35 ± 0.12 μs) is precisely the value expected for global rotational motion of MSL-S1 (Thomas et al., 1975). In the absence of nucleotide the ST-EPR spectrum of actin·MSL-S1 (Figure 2, rigor composite) shows that MSL-S1 is rotating slowly on the microsecond time scale, with a τ_r of 104 ± 14 μs. The observed submillisecond motions of the rigor complex are due entirely to flexibility within the actin filament, since τ_r is the same when the spin-label is attached to Cys-374 of actin rather than MSL-S1 (Thomas et al., 1979; Ostap & Thomas, 1991), and all of the myosin heads are bound to actin under these conditions. These results indicate that in the absence of nucleotide, MSL-S1 is bound rigidly to actin on the microsecond time scale. Upon the addition of 16 mM AMPPNP to actin + MSL-S1, the ST-EPR spectrum (Figure 2, AMPPNP composite) decreases slightly in intensity and changes shape, corresponding to a 4-fold decrease in τ_r (24.5 ± 5.5 μs). The effect of 5 mM ATPγS on the actin + MSL-S1 ST-EPR spectrum is much greater (Figure 2, ATPγS composite), resulting in a τ_r of 3.7 ± 1.8 μs.

The effective rotational correlation time (τ_r) of 24.5 μs, obtained for actin + MSL-S1 + AMPPNP (Figure 2, AMPPNP composite), is not an accurate characterization of the system, since the spectrum contains contributions from three species: actin·MSL-S1 (rigor), MSL-S1·AMPPNP (free), and actin·MSL-S1·AMPPNP (ternary complex). In order to obtain the spectrum of the ternary complex, we must subtract the other two spectra, weighted by their respective mole fractions as determined from the sedimentation experiments. Thus, in Figure 2, the ST-EPR spectrum of actin·MSL-S1·AMPPNP (AMPPNP bound) was obtained by subtracting 0.16 of the actin·MSL-S1 spectrum (rigor composite) and 0.22 of the MSL-S1·AMPPNP spectrum (AMPPNP free) from the spectrum of actin + MSL-S1 + AMPPNP (AMPPNP composite) and dividing by 0.62 to normalize the spectral intensity. This residual spectrum, with a τ_r of 115 ±7 μs, was not significantly different from the rigor actin·MSL-S1 spectrum (Figure 2, rigor composite). Thus MSL-S1·AMPPNP binds rigidly to actin, with no more microsecond rotational mobility than the rigor complex.

A ST-EPR spectrum of MSL-S1 bound to actin in the presence of ATPγS (Figure 2, ATPγS bound) was obtained in a similar manner, by subtracting 0.73 of the free MSL-S1 + ATPγS spectrum (Figure 2, ATPγS free) and dividing by 0.27 to normalize the spectral intensity. It was not necessary to correct for a rigor component, since ATPγS binds strongly enough to acto-S1 to saturate all of the myosin heads. The ST-EPR spectrum of the actin-attached myosin heads in the presence of ATPγS is quite different from the actin-attached myosin heads in rigor or in the presence of AMPPNP, which are not rotationally mobile on the microsecond time scale. On the contrary, actin-bound MSL-S1·ATPγS is quite mobile on the microsecond time scale, with a τ_r of 17 ± 2 μs.

At physiological ionic strength (μ = 186 mM), the ST-EPR spectra of acto-MSL-S1 (rigor) and MSL-S1 are identical to that at low ionic strength (data not shown). The ST-EPR spectra of actin + MSL-S1 + 16 mM AMPPNP (Figure 3, AMPPNP composite) indicates more mobility on the microsecond time scale than at μ = 100 mM, with a τ_r of 8.0 ± 2.3 μs. A ST-EPR spectrum of MSL-S1 bound to actin in the presence of AMPPNP at physiological ionic strength (Figure 3, AMPPNP bound) was obtained by subtracting 0.17 of the rigor acto-MSL-S1 spectrum and 0.58 of the MSL-S1 + AMPPNP spectrum from the acto-MSL-S1 + AMPPNP spectrum, and dividing by 0.25 to normalize the spectral intensity. The ST-EPR spectrum of the actin-attached myosin heads in the presence of AMPPNP at physiological ionic strength (Figure 3, AMPPNP bound) was not significantly different than the rigor acto-MSL-S1 spectrum (Figure 2, rigor composite), or the spectrum of the actin-bound MSL-S1 in

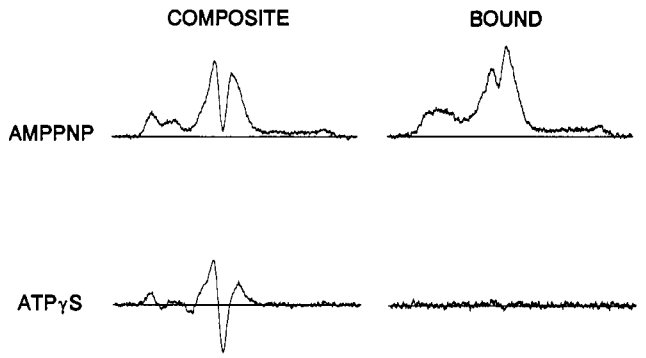

FIGURE 3: ST-EPR spectra of 100 μM MSL-S1 + 200 μM actin (left) and actin-bound MSL-S1 (right) in the presence of 16 mM AMPPNP (first row) or 5 mM ATPγS (second row) at μ = 186 mM, 25 °C. The spectra of the actin-bound MSL-S1 is that of the AMN ternary complex as determined from eqs 8 and 9 for AMPPNP and ATPγS, respectively. Each spectral baseline is 100 G wide.

the presence of AMPPNP at μ = 100 mM (Figure 2, AMPPNP bound), with a τ_r of 114 ± 5 μs. Thus MSL-S1·AMPPNP bound to actin is not rotationally mobile relative to actin on the microsecond time scale, and the observed decrease in τ_r upon increasing the ionic strength to 186 mM is due solely to an increase in the fraction of MSL-S1 detached from actin.

The ST-EPR spectrum of acto-MSL-S1 in the presence of 5 mM ATPγS (Figure 3, ATPγS composite) at physiological ionic strength (μ = 186 mM) is identical to that of free MSL-S1, with a τ_r of 0.42 ± 0.08 μs, as seen by the virtually flat residual after subtracting the MSL-S1 + ATPγS spectrum (Figure 3, ATPγS bound). This result is expected since the sedimentation binding experiments showed that none of the MSL-S1 is bound to actin at physiological ionic strength. This result supports the binding data that ATPγS binds strongly to acto-MSL-S1, saturating all of the myosin nucleotide binding sites.

Discussion

Summary of Results. We have used saturation-transfer electron paramagnetic resonance (ST-EPR), in conjunction with sedimentation binding experiments, to measure the microsecond rotational motions of actin-attached intermediate states of the myosin ATPase cycle. The ST-EPR spectrum of MSL-S1·AMPPNP bound to actin at low ionic strength (μ = 100 mM) is identical to that obtained in the absence of nucleotide (rigor complex), indicating no rotational motion of MSL-S1 relative to actin on the microsecond time scale. Increasing the ionic strength to physiological levels (μ = 186 mM) decreased the fraction of MSL-S1 bound to actin in the presence of AMPPNP but had no effect on the rotational mobility of the actin-attached myosin heads. However, MSL-S1·ATPγS bound to actin at low ionic strength (μ = 36 mM) is rotationally mobile, with an effective rotational correlation time (τ_r) of 17 ± 2 μs. At physiological ionic strength (μ = 36 mM) all of the MSL-S1 was dissociated from actin in the presence of ATPγS.

Interpretation of Binding Results. Determination of K_3, the association constant for MSL-S1 binding to actin in the presence of nucleotide, and K_4, the association constant for nucleotide binding to the acto-MSL-S1 complex, was essential in resolving the ST-EPR spectra of the actin-bound MSL-S1 in the presence of AMPPNP or ATPγS. In the presence of AMPPNP, the measured values of K_3 (2.23×10^4 M^{-1} at μ = 100 mM and 2.51×10^3 M^{-1} at μ = 186 mM) agreed closely with previous measurements made under similar conditions on unlabeled S1 (Green & Eisenberg, 1980a; Biosca et al., 1986; Duong & Reisler, 1987a). K_4 was determined to be approximately 3×10^2 M^{-1} at both ionic strengths for AMPPNP, in good agreement with previous measurements in solutions of acto-S1 (Biosca et al., 1986), myofibrils (Biosca et al., 1988), and muscle fibers (Pate & Cooke, 1985; Fajer et al., 1988). These values are thermodynamically consistent with the general binding scheme in Figure 1A. K_2, the association constant for S1 binding to actin in the absence of nucleotide, can be detemined from our values of K_3, K_4, and K_1, the association constant of AMPPNP for S1, by detailed balance (i.e., $K_1K_3 = K_2K_4$ or $K_2 = K_1K_3/K_4$). Using a value of 1.5×10^6 M^{-1} for K_1 (Greene & Eisenberg, 1980a) and our measured values of K_3 and K_4 we determined K_2 to be 1×10^8 M^{-1} at μ = 100 mM and 1×10^7 M^{-1} at μ = 186 mM, which are in good agreement with previously determined values of K_2 for unlabeled S1 under similar conditions (Greene & Eisenberg, 1980a; Biosca et al., 1986).

In the presence of ATPγS at μ = 36 mM, K_3 was determined to be 2.22×10^3 M^{-1}, which is consistent with previously measured values for unlabeled S1 (Goody & Hofmann, 1980; Geeves et al., 1986; Millar & Geeves, 1988). At μ = 186 mM, the binding of MSL-S1·ATPγS to actin was too weak to be measured, indicating that K_3 is less than 10^2 M^{-1} under these conditions. It was not necessary to measure K_4 for ATPγS, because the binding of ATPγS to acto-MSL-S1 was saturating, as shown by the [ATPγS]-independent value of K_{app}. This is consistent with the ability of 5 mM ATPγS to fully relax muscle fibers at physiological ionic strength, as determined by X-ray diffraction and mechanical measurements (Barrington-Leigh et al., 1972; Goody et al., 1975; Dantzig et al., 1988). The association constants measured in this work were determined directly on MSL-S1, under the conditions and protein concentrations used in the ST-EPR experiments. Since it was possible to determine K_3 and K_4 reliably under our experimental conditions, the quantitative analysis of the ST-EPR data to obtain the spectra of the ternary complexes (actin·MSL-S1·nucleotide) is valid.

Interpretation of AMPPNP ST-EPR Spectra. MSL-S1·AMPPNP bound to actin is rigidly attached, just as in the absence of nucleotide (rigor), with a τ_r of approximately 100 μs. The observed submillisecond rotational motions are due to flexibility within the actin filament and not to any microsecond rotational motions of the myosin head relative to actin, since the same motions are observed with MSL attached to Cys-374 on actin (Thomas et al., 1979; Ostap & Thomas, 1991). These results are consistent with a previous study of AMPPNP effects on the orientation and rotational motion of MSL-labeled myosin heads in muscle fibers (Fajer et al., 1988), in which it was shown that approximately half of the myosin heads in the presence of saturating AMPPNP are oriented and immobile on the microsecond time scale as in rigor, while the other half are detached and dynamically disordered as in relaxation. Cross-bridges in HMM (Greene, 1981; Duong & Reisler, 1987b) and in myofibrils (Chen & Reisler, 1984) are characterized by single-headed binding to actin in the presence of AMPPNP or ADP. ST-EPR studies of HMM (Manuck et al., 1986) and of myofibrils (Ishiwata et al., 1986) in the presence of AMPPNP have shown the same two populations of myosin heads observed in muscle fibers (Fajer et al., 1988). The results from the present work show that the myosin heads bound to actin in the presence of AMPPNP are the immobile population observed previously with HMM, myofibrils, and muscle fibers.

Since actin-attached myosin heads with AMPPNP bound have the same orientation and rotational rigidity as those in

rigor, or with ADP bound (Manuck et al., 1986; Fajer et al., 1990a), their conformation probably represents a strong binding state late in the actomyosin ATPase cycle. Biochemical evidence supports this conclusion, and mechanical and structural studies indicate that the AMPPNP state is probably intermediate between the ADP and relaxed states. The association constants of AMPPNP binding to myosin and actomyosin are closer to those of ADP than ATP (Greene & Eisenberg, 1978, 1980a), and S1 binds to regulated actin in the absence of Ca^{2+} with positive cooperativity in the presence of AMPPNP, just as in the presence of ADP, but not ATP (Greene, 1982; Williams & Greene, 1983). Experiments with cross-linked acto-S1 indicate that myosin heads in the presence of AMPPNP are structurally similar to those in the presence of ADP or in rigor (Duong & Reisler, 1989). However, electron microscopy coordinated with X-ray diffraction of insect flight muscle (Reedy et al., 1983, 1987), X-ray diffraction of vertebrate muscle (Lymn, 1975; Padron & Huxley, 1984), and EPR of spin-labeled myosin light chains in vertebrate muscle (Arata, 1990; Hambly et al., 1991) suggest that the distal (far from actin) portion of the myosin head is ordered with the thick filament, rather than the thin filament as in the ADP and rigor states. Cross-bridges in HMM (Greene, 1981; Duong & Reisler, 1987b) and in myofibrils (Chen & Reisler, 1984) are characterized by single-headed binding to actin in the presence of AMPPNP or ADP, in contrast to rigor cross-bridges which are bound to actin by both myosin heads (Eisenberg & Greene, 1980b). These results suggest that the AMPPNP state is structurally different from the ADP or rigor states and may represent an earlier state in the ATPase cycle. Mechanical measurements on muscle fibers in the presence of AMPPNP have also suggested that this state may represent a partial reversal of the power stroke (Marston et al., 1976; Kuhn, 1981), although cross-bridge detachment and reattachment to positions of lower strain cannot be ruled out in these experiments (Schoenberg, 1989). The ambiguity of cross-bridge attachment in the previous structural and mechanical experiments with AMPPNP makes it difficult to discern effects of cross-bridge detachment from changes in the actin-attached cross-bridge. In the present work, we have been able to differentiate the rotational motions of the actin-attached myosin heads from those arising from the dissociation of S1 from actin. *Thus, AMPPNP appears to trap myosin in a strong-binding intermediate state of the actomyosin ATPase cycle that is similar, but not identical, to the ADP and rigor states. It is clear, however, that these states late in the actomyosin ATPase cycle are rigidly bound to actin and not rotationally mobile (relative to actin) on the microsecond time scale.*

Interpretation of ATPγS ST-EPR Spectra. Myosin heads bound to actin in the presence of ATPγS have considerable microsecond rotational mobility, with an effective correlation time τ_r of 17 μs. Our results are consistent with X-ray diffraction of muscle fibers in the presence of ATPγS at low ionic strength, which indicate that the actin-attached cross-bridges are structurally distinct from rigor cross-bridges (Xu & Yu, 1991). In the presence of ATPγS at physiological or low ionic strengths, active muscle fibers develop stiffness without developing tension (Danzig et al., 1988), indicating that the myosin heads are in a weak-binding state early in the ATPase cycle that can bind to actin but can not generate force. These cross-bridges were found to have a range of measurable detachment rates, suggesting that multiple attached states may exist. Transitions between multiple attached states might account for the observed microsecond rotational motions of the ternary actin·MSL-S1·ATPγS complex, but time-resolved experiments will be necessary to test this hypothesis. Our results clearly demonstrate that in contrast to the later stages of the ATPase cycle, myosin heads in the presence of ATPγS are dynamically attached to actin, and this behavior in solution may be relevant to structural and mechanical properties of the muscle fiber.

We have previously reported that MSL-S1 bound to actin during steady-state hydrolysis of ATP at low ionic strength (μ = 36 mM) is rotationally mobile on the microsecond time scale, with an effective rotational correlation time τ_r of 1.0 ± 0.3 μs (Berger et al., 1989), which is much less than the value of τ_r measured in the presence of ATPγS (17 μs) in the present study. However, this apparent difference is due to the different spectral parameters measured. In the presence of ATP, only a few seconds were available for data acquisition, so the spectrum was monitored at a single spectral position (Berger et al., 1989). In the present study with ATPγS, several minutes were available for acquisition, permitting the analysis of the line-height ratio C'/C, which has been shown to be more reliable (Thomas et al., 1976). When the ATPγS spectrum was analyzed by the same procedure used in the ATP study, τ_r was determined to be 1.2 μs, in excellent agreement with the value obtained with ATP [1.0 μs, Berger et al. (1989)]. The different results obtained from different spectral parameters are probably due to the anisotropic motions S1 is likely to undergo, particularly when bound to actin (Squier et al., 1986). *Thus ATPγS induces anisotropic rotational motions of actin-bound S1 that are similar to those observed for actin-bound S1 during the steady state of actin-activated ATPase activity.* We found that the value of τ_r obtained from the normalized intensity parameter, which takes into account the entire EPR spectrum (Squier & Thomas, 1986), agrees with the value obtained using C'/C. *Thus our best estimate for the effective rotational correlation time of actin-attached MSL-S1 in the presence of ATPγS, or during the steady-state hydrolysis of ATP, is 17 μs.*

Since ATPγS is hydrolyzed by myosin approximately 500 times more slowly than is ATP (Bagshaw et al., 1972), it is believed to trap myosin in an early prehydrolysis intermediate of the actomyosin ATPase cycle that is probably similar to the actin·myosin·ATP state (Bagshaw et al., 1972; Barrington-Leigh et al., 1972; Goody et al., 1975). The predominant intermediate of the acto-S1 ATPase cycle during steady-state ATP hydrolysis is believed to be actin·myosin·ADP·Pi (Stein et al., 1985). The microsecond rotational motions of MSL-S1 bound to actin during the steady-state hydrolysis of ATP and in the presence of ATPγS are similar, with a τ_r of about 17 μs. *Thus, in contrast to strong-binding actin-attached intermediates of the myosin ATPase cycle (induced by AMPPNP, ADP, or rigor), which are immobile on the microsecond time scale and rigidly bound to actin, weakly bound actin-attached intermediates of the myosin ATPase cycle (induced by ATPγS, ATP, or ADP·Pi) have considerable microsecond rotational mobility.*

Alternative Explanations. An alternative explanation for the observed microsecond rotational motions of MSL-S1 bound to actin in the presence of ATPγS may be that the spin label becomes mobilized relative to the myosin head. While nucleotide binding to myosin has been known to mobilize certain SH_1-bound spin labels (Barnett & Thomas, 1987) and fluorescent probes (Thomas, 1987; Tanner et al., 1992), no difference was observed in the ST-EPR spectra of MSL-S1 in the absence of nucleotide or in the presence of AMPPNP or ATPγS, which all had a τ_r of 0.35 μs (Figure 2, Table II).

MSL-S1 has also been shown to remain rotationally rigid in the microsecond time range in the presence of ATP, as shown by the ST-EPR spectrum of MSL-S1 fixed on glass beads (Thomas et al., 1980). In order to determine more rigorously whether the whole myosin head is rotating and contributing to these motions, or just the domain around SH_1, it will be necessary to perform complementary experiments with the spin label at other sites on S1. We have previously considered the possibility that the S1 remains rigidly attached to actin even in the presence of ATP and that the nucleotide induces rotational motions in actin. Experiments using spin-labeled actin (at Cys-374), rather than S1, indicate that there is no change in the rotational mobility of actin during steady-state ATP hydrolysis (Ostap & Thomas, 1991). Therefore, we conclude that these motions are due to the rotation of S1 relative to actin.

In principle, the ST-EPR spectrum could also be affected by the rapid attachment/detachment equilibrium between S1 and actin, but the rate of detachment is slow enough that S1 spends 1–2 ms in the attached state with actin in the presence of ATP (White & Taylor, 1976) and even longer in the presence of ATPγS (Goody & Hofmann, 1980; Geeves et al., 1986) or AMPPNP (Marston, 1982; Trybus & Taylor, 1982). In order to affect the ST-EPR spectrum, the lifetime of the attached state would have to be comparable to or shorter than the spin–lattice relaxation time T_1, which is about 10 μs (Thomas et al., 1976). It is also possible that the accumulation of ADP following the hydrolysis of ATPγS affected the sedimentation binding and ST-EPR experiments. However, this is unlikely due to the extremely slow rate of hydrolysis of ATPγS by MSL-S1 (0.01 s^{-1}), which, like the MgATPase activity of S1, is slowed by spin labeling. At this rate, less than 10% of the ATPγS would be hydrolyzed by the end of the 10-min sedimentation binding experiments, and less than 50% by the end of even the longest ST-EPR experiments (typically lasting 45 min). No change was observed in the ST-EPR spectrum of acto-MSL-S1 in the presence of ATPγS from the first (5 min after adding ATPγS) to the last (45 min after adding ATPγS) scan acquired before digital averaging, indicating that the increasing concentration of ADP did not significantly affect the data.

The high concentrations of actin (200 μM) used in these experiments probably do not sterically restrict the rotation of S1 or artificially trap S1 in the actin filament lattice, since the ST-EPR spectrum of MSL-S1·ATPγS at physiological ionic strength is unaffected by 200 μM actin (Figure 3). While it is known that sulfhydryl modification at SH_1 partially inhibits the acto-S1 ATPase activity (Mulhern & Eisenberg, 1976, 1978; Svensson & Thomas, 1986), we believe the results obtained with spin-labeled myosin and its subfragments are applicable to unlabeled myosin as well. SH_1 modification does not affect the binding of S1 to actin significantly (Berger et al., 1989); the MSL-S1 ATPase can still actively cycle and is still activated by actin (Svensson & Thomas, 1986). Furthermore, the mechanical properties of muscle fibers spin-labeled at SH_1 are not significantly different from those of unlabeled muscle fibers (Crowder & Cooke, 1984; Barnett & Thomas, 1989; Fajer et al., 1991).

Relationship to EPR of Muscle Fibers. Complementary experiments in solution and in muscle fibers are important in examining the rotational mobility of myosin heads bound to actin during the active actomyosin ATPase cycle. The fraction of myosin heads bound to actin can be determined directly in solutions of S1 and actin and used to analyze the ST-EPR spectra explicitly in terms of the actin-attached component in the presence of different nucleotides. These results can then be used to interpret data obtained with muscle fibers, where it is not possible to determine unambiguously the fraction of actin-attached cross-bridges, and thus deconvolute the spectra in terms of an actin-attached component. Experiments with muscle fibers have established the relevance of the rotationally mobile actin-attached intermediate states of the myosin ATPase cycle in a more physiologically intact system.

Previous EPR studies on isometrically contracting muscle fibers have shown that less than 20% of the myosin heads are oriented as in rigor, while the rest are almost as highly disordered as in relaxation (Cooke et al., 1982; Fajer et al., 1990b). One interpretation of these results is that the disordered myosin heads are detached from actin, but an alternative explanation is that they are bound to actin in a rotationally dynamic state. The latter interpretation seems more likely since the stiffness of an isometrically contracting muscle fiber is 70–80% of the rigor value, indicating that most of the cross-bridges are attached to actin under these conditions (Fajer et al., 1990b). X-ray diffraction measurements on isometrically contracting muscle fibers also suggest that most of the myosin heads are associated with the thin filament (Haselgrove & Huxley, 1973). ST-EPR of isometrically contracting muscle fibers found the cross-bridges to be almost as mobile as in relaxation, with a τ_r of 25 μs, despite high stiffness values, indicating that the active cross-bridges are dynamically disordered (Barnett & Thomas, 1989). This value of τ_r is comparable to the τ_r of 17 μs measured in this work for myosin heads bound to actin in the presence of ATPγS and previously during the steady-state hydrolysis of ATP. The actual τ_r for the bound cross-bridges in the isometrically contracting muscle fiber is likely to be a bit longer, since some of the cross-bridges are certainly dissociated. This is to be expected, however, since the myosin heads in the muscle fiber will be more restricted by the myofibrillar lattice than S1 in solution. EPR (Fajer et al., 1990b) and time-resolved phosphorescence anisotropy (Stein et al., 1990) experiments indicate that the cross-bridge motions in an active isometric muscle fiber are not a linear combination of relaxed and rigor motions. This interpretation has been confirmed in this work and by Berger et al. (1989), *where the myosin heads have been unambiguously shown to be dynamically attached to actin, with a mobility that is intermediate between those of rigor and relaxation.*

Relationship to Other Work. We have identified a rotationally mobile state that is attached to actin during the myosin ATPase cycle that is distinct from the predominant states in rigor or relaxation. Evidence from other techniques supports this conclusion. X-ray diffraction on relaxed (Yu & Brenner, 1989) and isometrically contracting (Podolsky et al., 1976; Yu & Brenner, 1987) skeletal muscle fibers, and on bony fish muscle (Harford et al., 1991), have also identified an actin-attached cross-bridge state that is different from the rigor state, on the basis of changes in the radial mass distribution around the thick and thin filaments. Electron microscopy of cross-linked (Craig et al., 1985; Applegate & Flicker, 1987) and non-cross-linked solutions of actin and S1 (Trinick & White, 1991) or HMM (Frado & Craig, 1991), and of muscle fibers (Hirose et al., 1991), have shown that the myosin head is disordered while bound to actin in the presence of ATP. Disorder of the myosin heads while bound to actin, even in the muscle fiber, implies that myosin is quite flexible in its interaction with actin. Our results that S1 is rotationally mobile during attached states of the myosin ATPase cycle [this work and Berger et al. (1989)] are also consistent with results

obtained using the in vitro motility assay [Kron and Spudich (1986) and reviewed by Huxley (1990)], which has demonstrated that HMM is flexible enough to move actin filaments in opposite directions (Toyoshima et al., 1987) and that S1 alone is sufficient to move actin filaments (Toyoshima et al., 1989) and generate force on the actin filament comparable to that in a muscle fiber (Kishino & Yanagida, 1988). Since the myosin head only spends 1–2 ms at a given attachment site on actin (White & Taylor, 1976), submillisecond motions of S1 are required to move from one site of attachment on actin to another. Mechanical measurements on muscle fibers have shown that there are tension transients that follow a rapid stretch and release of the fiber during steady-state ATP hydrolysis, which probably arise from submillisecond rotations of actin-attached cross-bridges (Huxley & Simmons, 1971). Thus there is considerable structural and mechanical evidence to support the existence of a rotationally mobile actin-attached myosin head in the active cross-bridge cycle.

Previous structural (Barnett & Thomas, 1987; Shriver & Sykes, 1981, 1982) and kinetic [reviewed by Geeves et al. (1984) and Eisenberg and Hill (1985)] studies have suggested that there are two intrinsic conformations of S1, often termed the weakly and strongly bound intermediate states of the actomyosin ATPase cycle. The transition from the weakly to the strongly bound states has been postulated to be responsible for the mechanism of force generation in muscle (Eisenberg & Hill, 1985). In solution, although the weakly bound states are thought to be the predominant intermediates of the actomyosin ATPase cycle, they do not activate the thin filament or generate force (Stein et al., 1979; Brenner et al., 1982; Eisenberg & Hill, 1985). However, the actin-binding proteolytic fragment of caldesmon that specifically inhibits the formation of weakly bound cross-bridges, but not strongly bound ones that can generate force, has been shown to inhibit force production in active muscle fibers at physiological ionic strength, indicating that the weakly bound states are important intermediates in the process of force generation in the muscle fiber (Brenner et al., 1991). Despite high stiffness values, cross-bridges in relaxed muscle fibers at low ionic strength, which are predominantly in the weak binding conformation (Brenner et al., 1982), have been shown to be disordered and mobile on the microsecond time scale (Fajer et al., 1991). Similar results have been obtained in isometrically contracting muscle fibers at physiological ionic strength (Cooke et al., 1982; Barnett & Thomas, 1989; Stein et al., 1990; Fajer et al., 1990b), in which most of the cross-bridges are thought to be in the strong binding conformation (Goldman, 1987). Thus it is quite likely that the rotationally dynamic cross-bridges in an isometric muscle fiber are actively involved with the process of force generation.

Conclusions. We have demonstrated that spin-labeled myosin heads attached to actin in a ternary complex with ATPγS are rotationally mobile on the microsecond time scale, while those in a ternary complex with AMPPNP are not. The microsecond rotational motions of myosin heads attached to actin in the weakly bound intermediate states of the actomyosin ATPase cycle that occur both in the presence of ATPγS and during the steady-state hydrolysis of ATP (Berger et al., 1989) are probably intimately involved in the process of force generation within the muscle fiber as well. Similar cross-bridge motions have been identified in isometrically contracting muscle fibers (Barnett & Thomas, 1989; Fajer et al., 1990b), but it remains to be determined whether the rotationally mobile myosin heads correspond only to the weakly bound states preceding force generation or to the actual force generating states as well. Future experiments using time-resolved spectroscopic techniques, in conjunction with transient biochemical and mechanical pertubations of the contractile cycle, will be required to correlate more precisely the microsecond rotational motions of actin-attached cross-bridges with the underlying mechanism of muscle contraction.

ACKNOWLEDGMENTS

Eric C. Svensson carried out preliminary experiments that led to this study. We thank E. Michael Ostap and James E. Mahaney for critically reading the manuscript, Richard A. Stein and John J. Matta for helpful discussions, Pierre Hilo, Robert Decker, Robert L. H. Bennett, and Franz Nisswandt for technical assistance, and Timothy Walseth, Karl Olson, and William Schroeder for their assistance in purifying the nucleotide analogues.

Registry No. ATPase, 9000-83-3; AMPPNP, 25612-73-1; ATPγS, 35094-46-3.

REFERENCES

Applegate, D., & Flicker, P. (1987) *J. Biol. Chem. 262*, 6856–6863.

Arata, T. (1990) *J. Mol. Biol. 214*, 471–478.

Bagshaw, C. R., Eccleston, J. F., Trentham, D. R., & Yates, D. W. (1972) *Cold Spring Harbor Symp. Quant. Biol. 37*, 127–135.

Barnett, V. A., & Thomas, D. D. (1987) *Biochemistry 26*, 314–323.

Barnett, V. A., & Thomas, D. D. (1989) *Biophys. J. 56*, 517–523.

Barrington-Leigh, J., Holmes, K. C., Mannherz, H. G., Rosenbaum, G., Eckstein, F., & Goody, R. S. (1972) *Cold Spring Harbor Symp. Quant. Biol. 37*, 443–448.

Berger, C. L., Svensson, E. C., & Thomas, D. D. (1989) *Proc. Natl. Acad. Sci. U.S.A. 86*, 8753–8757.

Biosca, J. A., Greene, L. E., & Eisenberg, E. (1986) *J. Biol. Chem. 261*, 9793–9800.

Biosca, J. A., Greene, L. E., & Eisenberg, E. (1988) *J. Biol. Chem. 263*, 14231–14235.

Brenner, B., Schoenberg, M., Chalovich, J. M., Greene, L. E., & Eisenberg, E. (1982) *Proc. Natl. Acad. Sci. U.S.A. 79*, 7288–7291.

Brenner, B., Yu, L. C., & Chalovich, J. M. (1991) *Proc. Natl. Acad. Sci. U.S.A. 88*, 5739–5743.

Chalovich, J. M., & Eisenberg, E. (1982) *J. Biol. Chem. 257*, 2432–2437.

Chen, T., & Reisler, E. (1984) *Biochemistry 23*, 2400–2407.

Cooke, R., Crowder, M. S., & Thomas, D. D. (1982) *Nature 300*, 776–778.

Craig, R., Greene, L. E., & Eisenberg, E. (1985) *Proc. Natl. Acad. Sci. U.S.A. 82*, 3247–3251.

Crowder, M. S., & Cooke, R. (1984) *J. Muscle Res. Cell Motil. 5*, 131–146.

Danzig, J. A., Walker, J. W., Trentham, D. R., & Goldman, Y. E. (1988) *Proc. Natl. Acad. U.S.A. 85*, 6716–6720.

Duong, A. M., & Reisler, E. (1987a) *J. Biol. Chem. 262*, 4124–4128.

Duong, A. M., & Reisler, E. (1987b) *J. Biol. Chem. 262*, 4129–4133.

Duong, A. M., & Reisler, E. (1989) *Biochemistry 28*, 3502–3509.

Eads, T. M., Thomas, D. D., & Austin, R. H. (1984) *J. Mol. Biol. 179*, 55–81.

Eisenberg, E., & Hill, T. L. (1985) *Science 227*, 999–1006.

Fajer, P. G., Fajer, E. A., Brunsvold, N. J., & Thomas, D. D. (1988) *Biophys. J. 53*, 513–524.

Fajer, P. G., Fajer, E. A., Matta, J. M., & Thomas, D. D. (1990a) *Biochemistry 29*, 5865–5871.
Fajer, P. G., Fajer, E. A., & Thomas, D. D. (1990b) *Proc. Natl. Acad. Sci. U.S.A. 87*, 5538–5542.
Fajer, P. G., Fajer, E. A., Schoenberg, M., & Thomas, D. D. (1991) *Biophys. J.* (in press).
Frado, L., & Craig, R. (1991) *Biophys. J. 59*, 429a.
Geeves, M. A., Goody, R. S., & Gutfreund, H. (1984) *J. Muscle Res. Cell Motil. 5*, 351–361.
Geeves, M. A., Jeffries, T. E., & Millar, N. C. (1986) *Biochemistry 25*, 8454–8458.
Goldman, Y. E. (1987) *Annu. Rev. Physiol. 49*, 637–654.
Goody, R. S., & Hofmann, W. (1980) *J. Muscle Res. Cell Motil. 1*, 101–115.
Goody, R. S., Holmes, K. C., Mannherz, H. G., Barrington-Leigh, J., & Rosenbaum, G. (1975) *Biophys. J. 15*, 687–705.
Greene, L. E. (1981) *Biochemistry 20*, 2120–2126.
Greene, L. E. (1982) *J. Biol. Chem. 257*, 13993–13999.
Greene, L. E., & Eisenberg, E. (1978) *Proc. Natl. Acad. Sci. U.S.A. 75*, 54–58.
Greene, L. E., & Eisenberg, E. (1980a) *J. Biol. Chem. 255*, 543–548.
Greene, L. E., & Eisenberg, E. (1980b) *J. Biol. Chem. 255*, 549–554.
Hambly, B., Franks, K., & Cooke, R. (1991) *Biophys. J. 59*, 127–138.
Harford, J., Squire, J., Chew, M., & Towns-Andrews, L. (1991) *Biophys. J. 59*, 575a.
Haselgrove, J. C., & Huxley, H. E. (1973) *J. Mol. Biol. 77*, 549–568.
Hirose, K., Lenart, T. D., Franzini-Armstrong, C., & Goldman, Y. E. (1991) *Biophys. J. 59*, 577a.
Huxley, A. F. (1974) *J. Physiol. 243*, 1–43.
Huxley, A. F., & Simmons, R. M. (1971) *Nature 233*, 533–538.
Huxley, H. E. (1969) *Science 114*, 1356–1366.
Huxley, H. E. (1990) *J. Biol. Chem. 265*, 8347–8350.
Huxley, H. E., & Kress, M. (1985) *J. Muscle Res. Cell. Motil. 6*, 153–162.
Ishiwata, S., Manuck, B. A., Seidel, J. C., & Gergely, J. (1986) *Biophys. J. 49*, 821–828.
Kishino, A., & Yanagida, T. (1988) *Nature 334*, 74–76.
Kron, S. J., & Spudich, J. A. (1986) *Proc. Natl. Acad. Sci. U.S.A. 83*, 6272–6276.
Kuhn, H. J. (1981) *J. Muscle Res. Cell. Motil. 2*, 7–44.
Lanzetta, P. A., Alvarez, L. J., Reinach, P. S., & Candia, O. A. (1979) *Anal. Biochem. 100*, 95–97.
Lymn, R. W. (1975) *J. Mol. Biol. 99*, 567–582.
Lymn, R. W., & Taylor, E. W. (1971) *Biochemistry 10*, 4617–4624.
Manuck, B. A., Seidel, J. C., & Gergely, J. (1986) *Biophys. J. 50*, 221–230.
Marston, S. B. (1982) *Biochem. J. 203*, 453–460.
Marston, S. B., Rodger, C. D., & Tregear, R. T. (1976) *J. Mol. Biol. 104*, 263–276.
Millar, N. C., & Geeves, M. A. (1988) *Biochem. J. 249*, 735–743.
Mulhern, S. A., & Eisenberg, E. (1976) *Biochemistry 15*, 5702–5708.
Mulhern, S. A., & Eisenberg, E. (1978) *Biochemistry 17*, 4419–4425.
Ostap, E. M., & Thomas, D. D. (1991) *Biophys. J. 59*, 1235–1241.
Padron, R., & Huxley, H. E. (1984) *J. Muscle Res. Cell Motil. 5*, 613–655.
Pate, E., & Cooke, R. (1985) *Biophys. J. 47*, 773–780.
Pate, E., & Cooke, R. (1988) *Biophys. J. 53*, 561–573.
Podolsky, R. J., St. Onge, R., Yu, L., & Lymn, R. W. (1976) *Proc. Natl. Acad. Sci. U.S.A. 73*, 813–817.
Reedy, M. C., Reedy, M. K., & Goody, R. S. (1983) *J. Muscle Res. Cell. Motil. 4*, 55–81.
Reedy, M. C., Reedy, M. K., & Goody, R. S. (1987) *J. Muscle Res. Cell. Motil. 8*, 473–503.
Schoenberg, M. (1989) *Biophys. J. 56*, 33–41.
Shriver, J. W., & Sykes, B. D. (1981) *Biochemistry 20*, 2004–2012.
Shriver, J. W., & Sykes, B. D. (1982) *Biochemistry 21*, 3022–3028.
Squier, T. C., & Thomas, D. D. (1986) *Biophys. J. 49*, 921–935.
Stein, L. A., Greene, L. E., Chock, P. B., & Eisenberg, E. (1985) *Biochemistry 24*, 1357–1363.
Stein, R. A., Ludescher, R. D., Dahlberg, P. S., Fajer, P. G., Bennett, R. L. H., & Thomas, D. D. (1990) *Biochemistry 29*, 10023–10031.
Svensson, E. C., & Thomas, D. D. (1986) *Biophys. J. 50*, 999–1002.
Tanner, J. W., Thomas, D. D., & Goldman, Y. E. (1992) *J. Mol. Biol.* (in press).
Thomas, D. D. (1987) *Annu. Rev. Physiol. 49*, 691–709.
Thomas, D. D., Seidel, J. C., Hyde, J. S., & Gergely, J. (1975) *Proc. Natl. Acad. Sci. U.S.A. 72*, 1729–1733.
Thomas, D. D., Dalton, L. R., & Hyde, J. (1976) *J. Chem. Phys. 65*, 3006–30024.
Thomas, D. D., Seidel, J. C., & Gergely, J. (1979) *J. Mol. Biol. 132*, 257–273.
Thomas, D. D., Ishiwata, S., Seidel, J. C., & Gergely, J. (1980) *Biophys. J. 32*, 873–890.
Toyoshima, Y. Y., Kron, S. J., McNally, E. M., Niebling, K. R., Toyoshima, C., & Spudich, J. A. (1987) *Nature 328*, 536–539.
Toyoshima, Y. Y., Toyoshima, C., & Spudich, J. A. (1989) *Nature 341*, 154–156.
Trinick, J., & White, H. (1991) *Biophys. J. 59*, 410a.
Trybus, K. M., & Taylor, E. W. (1982) *Biochemistry 21*, 1284–1294.
White, H. D., & Taylor, E. W. (1976) *Biochemistry 15*, 5818–5826.
Williams, D. L., & Greene, L. E. (1983) *Biochemistry 22*, 2770–2774.
Xu, S., & Yu, L. C. (1991) *Biophys. J. 59*, 575a.
Yount, R. G., Babcock, D., Ballantyne, W., & Ojala, D. (1971a) *Biochemistry 10*, 2484–2489.
Yount, R. G., Ojala, D., & Babcock, D. (1971b) *Biochemistry 10*, 2490–2496.
Yu, L. C., & Brenner, B. (1987) *Biophys. J. 51*, 473a.
Yu, L. C., & Brenner, B. (1989) *Biophys. J. 55*, 441–453.